3D multimodal simulation of image acquisition by X-Ray and MRI for validation of seedling measurements with segmentation algorithms

Landry Benoit[1], Georges Semaan[1], Florence Franconi [2],
Étienne Belin[1], François Chapeau-Blondeau[1],
Didier Demilly[3], David Rousseau[4]

(1) Laboratoire Angevin de Recherche en Ingénierie des Systèmes (LARIS),
Université d'Angers, 62 avenue Notre Dame du Lac, 49000 Angers, France.
(2) Plateforme d'Ingénierie et d'Analyse Moléculaire (PIAM), Université d'Angers.
(3) GEVES, Station Nationale d'Essais de Semences (SNES),
rue Georges Morel, 49071 Beaucouzé, France.
(4) Université de Lyon, Laboratoire CREATIS; CNRS, UMR5220; INSERM, U1044;
Université Lyon 1; INSA-Lyon, 69621 Villeurbanne, France.

Abstract. In this report, we present a 3D simulator for the numerical validation of segmentation algorithms for seedling in soil from X-ray or MRI. A 3D simulator of root in elongation is coupled to a simulator of the image acquisition to generate images of simulated seedling associated with a known synthetic ground truth. We detail how acquisition parameters of the seedling and parameters of the imaging systems are estimated and combined to produce realistic images. The resulting simulator is available on line to open the possibility of segmentation challenges with *in silico* validation based on unlimited number of seedling.

Keywords: Seedling monitoring, X-Ray, MRI, 3D simulation.

1 Introduction

Plant roots present challenges for computer vision, as they form rich 3D networks inaccessible via visible light imaging. Analysis of these highly complex structures has recently been made possible in 3D and directly in pots with soil by the use of X-Ray computed tomography (X-Ray CT)[1–3] or magnetic resonance imaging (MRI) [4]. In addition, the constitution of roots and soil in terms of atomic number and water composition are often poorly contrasted in X-Ray CT or MRI, making the segmentation of such images also challenging. Accordingly, the segmentation of the roots from X-Ray CT or MRI is currently receiving attention from computer scientists, to develop new algorithms [1–4]. Because of their novelty, these first segmentation algorithms of [1–4] stand as pilot studies and proofs of feasibility. However, the assessment of performance of such image processing tasks is uneasy. Mechanical extraction of the root from the soil for topological comparison is risky since it might damage or destruct the smallest parts of the root system. Also, since X-Ray CT and MRI are rather new as routine tools for plant science, it is complicated to find experts in plant science and radiology to manually segment the root in 3D as commonly done in X-Ray CT and MRI for the segmentation of organs in the biomedical domain. Another approach, usual in the biomedical domain, and here also difficult to transpose to plant science because of the network nature of the roots, is the realization of physical phantoms. In this report, we propose an alternative for the validation of segmentation algorithms from X-Ray CT and MRI with the use of a 3D root simulator coupled to a simulator of the image acquisition to generate 3D stacks of X-ray like or MRI like images of simulated plants associated with a known synthetic ground truth. Such an approach is quite common again in the biomedical domain [5], but has only very recently been introduced to roots [4, 6]. The proposed numerical validation method of algorithms for image processing of roots described in Fig. 1 is composed of three stages: A seedling simulator establishes a ground truth. This is followed by an acquired image simulator which generates the images to be processed by the algorithm being tested. At the end, a comparison between the ground truth and the results produced by the algorithm is realized. The imaging system simulated in [6] generates seedling

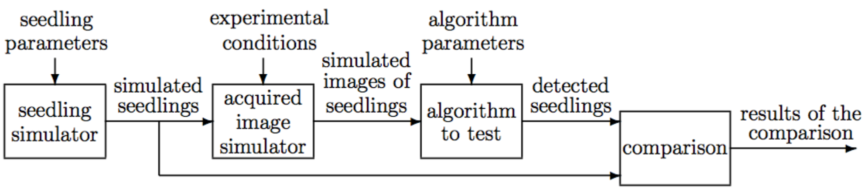

Fig. 1. Principle of the numerical method used to validate image processing algorithms of seedling images. In this report we present the coupling between a 3D seedling simulator with two acquired image simulator: X-ray CT and MRI.

in 2D acquired from backlight with conventional visible imaging. We provide an extension of [6] in 3D and apply it to X-Ray CT and MRI. The monitoring of the elongation of seedling is an important biological task since this elongation corresponds to the so-called heterotrophic growth which is highly correlated with the probability of emergence of the seedling at the surface of the soil. Also, the analysis of movement of the radicle of seedling during the elongation stage has recently been demonstrated to reveale oscillations of the tip of the root. Such findings are of great interest for bio-inspired robotics [7], however, so far the analysis of these oscillatory movements have been demonstrated outside the soil. This adds another motivation for the segmentation of the seedling in the soil and the importance to validate the segmentation algorithms with the simulation approach presented in this report.

The report is organized as follows. We start with the simulator of seedling and then give the image acquisition simulator used for X-Ray CT and MRI. This is illustrated with simulated images of various plants at the scale of seedlings. We present how simulation tools introduced for the biomedical domain in [5] for X-Ray CT and MRI can be also serve for plants. We eventually discuss possible extensions of this work and provide the address of the on line platform to run our simulator.

2 Seedling elongation simulation

Seedling are simulated from the L-system process described in [8] which enables accelerated elaboration of root systems simulated in 3D with no control on root width as shown in Fig. 2. We use the upgraded version of this simulator recently presented in [6] which allows, as visible in Fig. 3, the generation of spherical seeds at initial time and adds control on root width. This seedling simulator is available on line at [9]. This corresponds to the germination and elongation stages of seedling growth occuring for real plants in the soil before the activation of the photosynthesis. The parameters used by this simulator are the size of the seeds, the width of the roots, the number of roots per seedling and the duration of the simulation fixing the overall size of the root system.

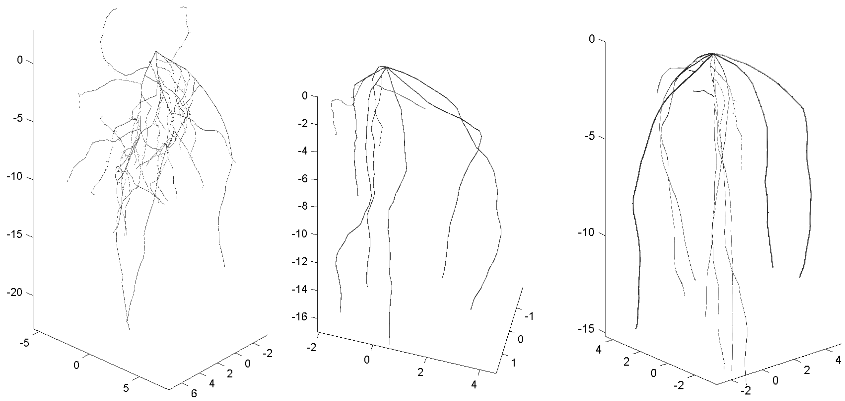

Fig. 2. Three simulated root systems using the generation algorithm described in [8].

3 Image simulator

The simulation of images of seedling acquired by a specific imaging technique requires the estimation of the physical parameters at the origin of the contrasts

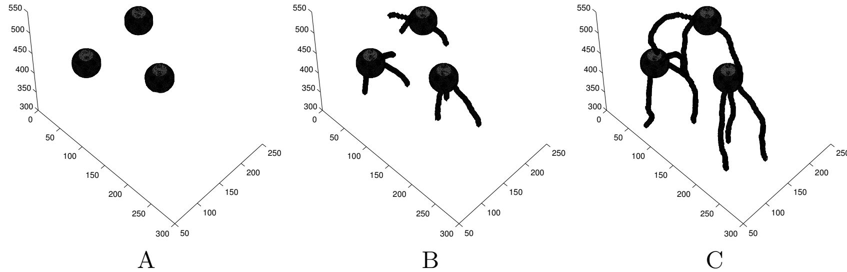

Fig. 3. Three simulated seedlings in phase of elongation from the stage of seeds (A), at 7 days (B), at 14 days (C) with the simulator described in [6] and extended here in 3D. After the initial time the spheres gives rise to the cotyledons and the tubular parts to the radicles of the seedling.

in the images produced by this imaging technique. We start with X-Ray CT which provides, in first approximation, a contrast of absorbance of X-Ray in the tissue following a Beer-Lambert exponential law as a function of the width x of the sample

$$I(x) = I_0 \exp(-\mu x) \ , \tag{1}$$

with I_0 the intensity of the incident X-Ray beam and μ, expressed in m^{-1}, the absorbance coefficient. With prior knowledge of I_0 and seedling width x, we estimated from the X-Ray 2D projection of Fig. 4 (obtained for a given and fixed beam energy), the absorbance μ in the seedlings, assumed here in first approximation as homogeneous, for various species. We then recorded images of a pot containing only the nutritive substrate where the seedling are to grow. For illustration, two substrates of practical interest were acquired with sand and soil. The resulting tomogram displays complex 3D structures at multiple scales difficult to reproduce with simple statistical models such as surrogates models based on first and second order statistics. Instead, we propose, as in [6] and shown in Fig. 5, an empirical approach by recording a bank of images of real substrate. It is then straightforward to generate, as in Fig. 6, simulation of images of a seedling in substrate by replacing the background of the seedling by the substrate and by simulating the intensity in the seedling from Eq. (1). To appreciate the realism of our simulator, we provide in Fig. 7 two views of a seedling in soil and sand acquired from a real X-Ray system. Fig. 6 and 7 demonstrate that the segmentation of seedling in soil is a difficult problem for plant image analysis. The segmentation of root in soil in X-Ray CT images has been recently solved with an elegant region growing approach based on the Shannon-Jensen divergence [1–3]. The segmentation in these studies is done on adult plants with aerian parts highly contrasted in X-Ray CT. Therefore it is easy to locate the position of the root at the surface of the soil as initiation of the region-growing process. Such an initiation is more difficult to realize automatically or manually when one works on seeds or seedling buried in the soil. Consequently, the segmentation of X-Ray CT images of seedling in soil stands as an open problem for plant phenotyping that can be tackled with *in silico* validation with the simulation approach with have initiated here.

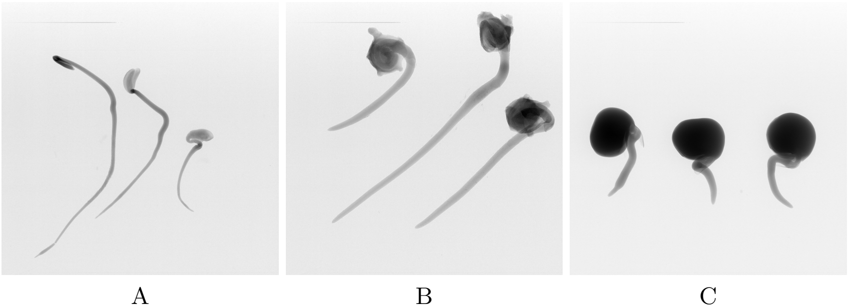

Fig. 4. X-Ray images of *Medicago truncatula* (A), sugar beet (B) and peas (C). The mesurated absorbance of cotyledons is 366±34 m^{-1} for *Medicago truncatula*, 338±27 m^{-1} for sugar beet and 166±12 m^{-1} for Peas. The mesurated absorbance of radicle is 372±74 m^{-1} for *Medicago truncatula*, 428±13 m^{-1} for sugar beet and 271±29 m^{-1} for Peas.

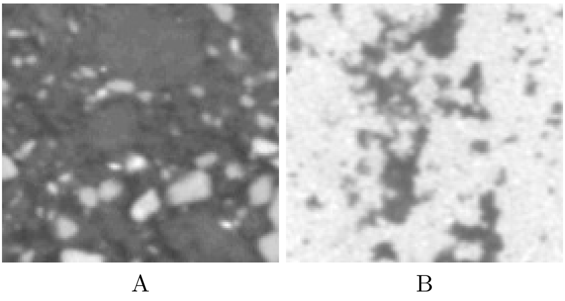

Fig. 5. Two experimentally acquired X-Ray tomography images of substrate for the seedling (A: a pot of soil - B: a pot of sand with water).

We have undertaken the same approach of 3D simulator with MRI that we now describe in a similar way. Basic spin-echo MRI sequences provide a gray level I in the tissue depending on the density of protons DP, relaxation times (T_1, T_2) and acquisition times T_R (repetition time) and T_E (acquisition time) in

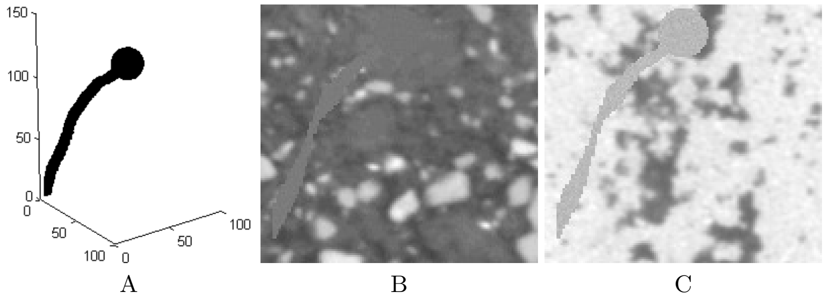

Fig. 6. 3D simulated seedling (A) used as ground truth to simulate the X-Ray CT images of B and C respectively produced with the substrates of Figs. 5A and B.

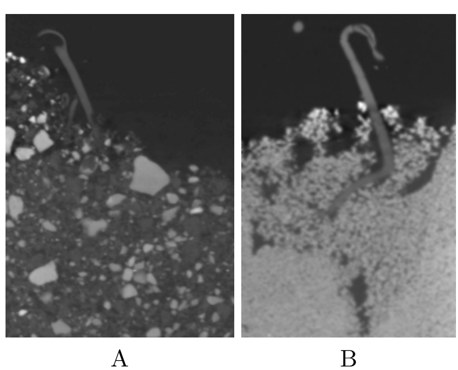

Fig. 7. Two experimentally acquired X-Ray tomography images of wheat seedlings in a pot of soil (A) and in a pot of sand (B).

response to magnetic impulses following

$$I \sim DP \times [1 - \exp((-T_R)/T_1)] \exp((-T_E)/T_2) \; . \quad (2)$$

Contrasts in basic spin-echo MRI therefore depends on characteristics (DP, T_1, T_2) and acquisition parameters (T_E, T_R). For illustration, we have estimated these parameters modeled as Gaussian distributions in seedlings of wheat buried in sand with water. The corresponding estimates are given in Table 1.

Parameters	T1 (in milliseconds)	T2 (in milliseconds)	DP
Water in sand	$m = 2626$; $std = 86$	$m = 17$; $std = 5$	$m = 65912$; $std = 1443$
Cotyledons	$m = 989$; $std = 44$	$m = 17$; $std = 5$	$m = 123187$; $std = 29341$
Radicle	$m = 2235$; $std = 47$	$m = 34$; $std = 1$	$m = 250304$; $std = 5597$

Table 1. Mean m, and standard deviation std for MRI parameters of Eq. (2) estimated from averaging on seedlings of wheat in sand with water. Acquisition realized on a Bruker Advance DRX MRI system (Bruker Biospin SA, Wissembourg, France) in conventional acquisition conditions with a reference 2D spin-echo and a linear sampling process.

Therefrom, based on the binary masks of simulated seedlings such as those of Fig. 3, we can generate 3D maps of MRI parameters (DP, T_1, T_2) here modeled as Gaussian distribution with mean and standard deviation values taken from Table 1 in the sand (background), the cotyledons (sphere) and the radicle (tubular part). The simulation of 2D spin-echo MRI images can then be obtained from the computation of Eq. (2) for a choice of acquisition parameters (T_R, T_E). This can be done automatically on line with help of the virtual imaging platform VIP [5]. It is then possible to search for optimal acquisition parameters (T_R, T_E) for a given image processing tasks. A very useful simulation tool indeed since the choice of acquisition parameters are usually left to the qualitative empirical expertise of the person in charge of the acquisition but without guarantee of satisfying an optimal criterion on the information to be eventually extracted from the images. As an illustration of the interest of our simulation process, we give in Fig. 8 the MRI images generated from different choices of acquisition parameters (T_R, T_E). To appreciate the realism of our simulator, we provide in Fig. 9 a view of a seedling buried in sand with water acquired from a real MRI system with similar acquisition parameters. Simulation of root systems in MRI were also given in [4], but it is to be noted that the approach was distinct from the one described above. In [4], the MRI signal in the substrate and in the root system is generated with a statistical approach from a Gaussian model in the acquired image I directly (while our Gaussian model lay here on (DP, T_1, T_2)) and tested for various signal to noise ratio (SNR). Here, the proposition is more physics-oriented with the simulation of the 2D spin-echo signal which allow to search for the acquisition parameters giving the optimal SNR.

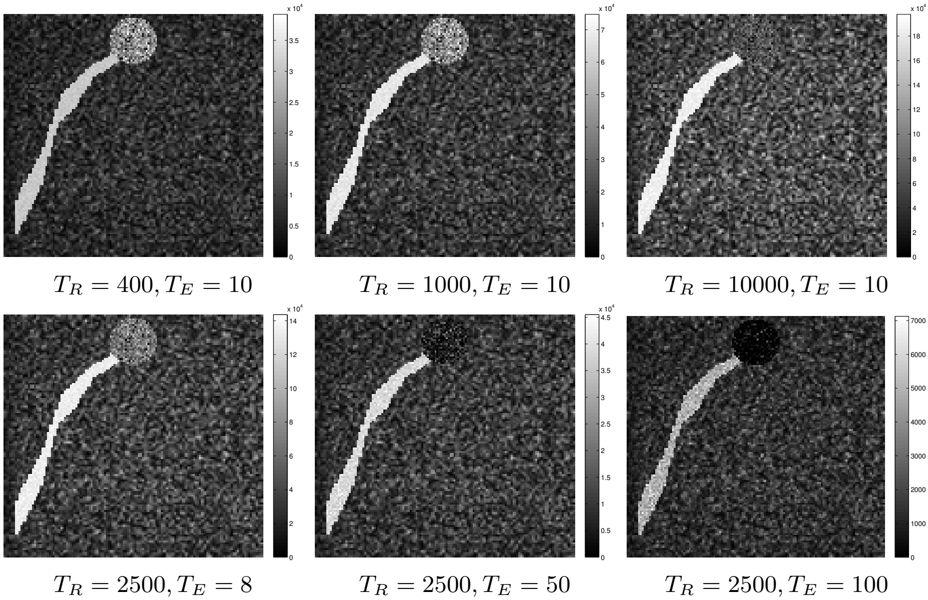

Fig. 8. Six MRI images generated from different choices of acquisition parameters (T_R, T_E). The gray scale level is different from one image to another in order to facilitate visualization.

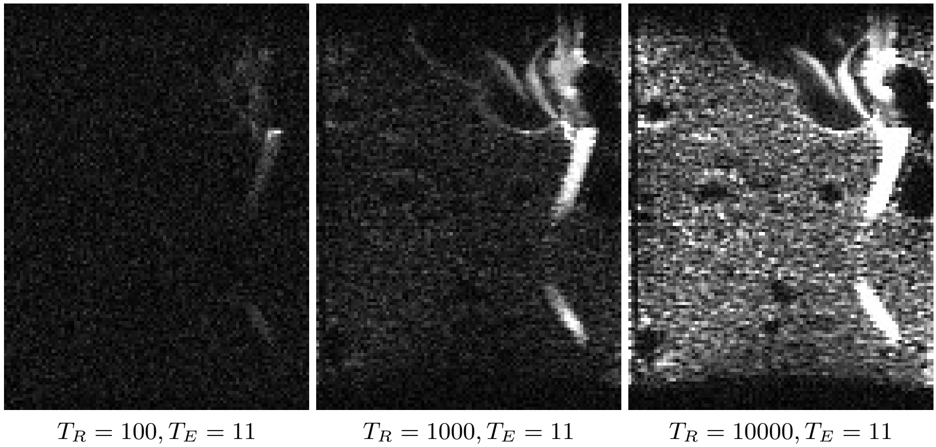

Fig. 9. Three images of a seedling of wheat in a pot of sand acquired from a real MRI system with different choices of acquisition parameters (T_R, T_E).

4 Conclusion

We have extended to 3D and multimodality the simulation approach recently introduced in [6] for *in silico* validation of root segmentation algorithms. The simulator in [6] was given in 2D and illustrated with seedling segmentation from visible imaging in backlight mode. Our new simulator can now serve for the validation, with a 3D synthetic ground truth, of root segmentation algorithms applied on 3D images of roots. For illustration here we have generated images of seedlings in substrate of soil or sand. The acquisition parameters for X-Ray CT or MRI in the seedling were considered spatialy homogeneous or distributed following Gaussian distributions. It would however be straightforward to inject more elaborated spatial variation models on larger root systems if a more realistic description is needed. Other perspectives concern the extension to other imaging modalities of interest for root screening. This includes 3D positron emission tomography (PET) which gives access to physiological informations in roots [10]. The estimation of desintegration life-time of biomarkers would have to be undertaken but the virtual imaging platform [5] used in this report for MRI also incorporates PET simulation and could thus still serve to generate simulated images. Also, when the full 3D organization of the roots or the mechanical impact of the soil on the root are not required for the biological purpose, it is possible to lower the cost of the imaging modality and use rhizotron or hydroponic growth in which roots are accessible from conventional visible imaging. These imaging systems however present specificities due to the presence of a nutritive substrate possibly different from the one modeled in [6] and it would also be interesting to extend our simulation approach to these systems.

Acknowledgment

This work received support from the French Government supervised by the "Agence Nationale de la Recherche" in the framework of the program "Investissements d'Avenir" under reference ANR-11-BTBR-0007 (AKER program). Landry BENOIT gratefully acknowledges financial support from Angers Loire Métropole and SNES-GEVES for the preparation of his PhD. Authors thank Lydie Ledroit (INRA) for technical support on seedlings, Karima Boudehri and Laurence Lecorre from SNES-GEVES for X-Ray acquisition on the platform PHENOTIC, Angers, France and Sorina Pop from CREATIS, Université Lyon 1, France for introducing to simulation on the platform VIP.

References

1. Mairhofer, S., Zappala, S., Tracy, S., Sturrock, C., Bennett, M., Mooney, S., Pridemore, T.: Rootrak: automated recovery of 3D plant root architecture in soil with X-Ray micro computed tomography using visual tracking. Plant Physiology **158** (2012) 561–569
2. Zappala, S., Mairhofer, S., Tracy, S., Sturrock, C., Bennett, M., Pridemore, T., Mooney, S. Quantifying the effect of soil moisture content on segmenting root system architecture in X-Ray micro-Computed Tomography. Plant and Soil (2013)
3. Mairhofer, S., Zappala, S., Sturrock, C., Bennett, M., Mooney, S., Pridemore, T. Recovering complete plant root system architectures from soil via X-Ray Micro-Computed Tomography. Plant Physiology **359** (2013)
4. Schultz, H., Postma, J., Dusschoten, D., Scharr, H., Behnke, S.: Plant root system from MRI images. Computer Vision, Imaging and Computer Graphics **359** (2013) 411–425
5. Glatard, T., Lartizien, C., Gibaud, B., Ferreira da Silva, G.,Cervenansky, F., Alessandrini, M., Benoit Cattin, H., Bernard, O.,Camarasu Pop, S.: A virtual imaging platform for multi-modality medical image simulation. IEEE Transactions on Medical Imaging **32** (2013) 110–118
6. Benoit, L. Rousseau, D., Belin, E., Demilly, D., Chapeau Blondeau, F.: Simulation of image acquisition in machine vision dedicated to seedling elongation to validate image processing root segmentation algorithms. Computers and Electronics in Agriculture **104** (2014) 84–92
7. Popova, L., Russino, A., Ascrizzi, A., Mazzolai, B.: Analysis of movement in primary maize roots. Biologia **67** (2012) 517–524
8. Leitner, D., Klepsch, S., Bodner, G., Schnepf, A.: A dynamic root system growth model based on L-systems. Plant Soil **332** (2010) 177–192
9. http://lisabiblio.univ-angers.fr/PHENOTIC/telechargements.html
10. Jahnke, S. and Menzel, M. I. and Van Dusschoten, D. and Roeb, G. W. and Bühler, J. and Minwuyelet, S. and Blümler, P. and Temperton, V. M. and Hombach, T. and Streun, M. and Beer, S. and Khodaverdi, M. and Ziemons, K. and Coenen, H. H. and Schurr, U.: Combined MRI-PET dissects dynamic changes in plant structures and functions. Plant Journal **59** (2009) 634–644